

A SINGLE GRAPH CONVOLUTION IS ALL YOU NEED: EFFICIENT GRAYSCALE IMAGE CLASSIFICATION

Jacob Fein-Ashley[†], Tian Ye[†], Sachini Wickramasinghe[†], Bingyi Zhang[†], Rajgopal Kannan^{*}, Viktor Prasanna[†]

[†] University of Southern California, ^{*}DEVCOM Army Research Lab

ABSTRACT

Image classifiers often rely on convolutional neural networks (CNN) for their tasks, which are inherently more heavyweight than multilayer perceptrons (MLPs), which can be problematic in real-time applications. Additionally, many image classification models work on both RGB and grayscale datasets. Classifiers that operate solely on grayscale images are much less common. Grayscale image classification has diverse applications, including but not limited to medical image classification and synthetic aperture radar (SAR) automatic target recognition (ATR). Thus, we present a novel grayscale (single channel) image classification approach using a vectorized view of images. We exploit the lightweightness of MLPs by viewing images as a vector and reducing our problem setting to the grayscale image classification setting. We find that using a single graph convolutional layer batch-wise increases accuracy and reduces variance in the performance of our model. Moreover, we develop a customized accelerator on FPGA for the proposed model with several optimizations to improve its performance. Our experimental results on benchmark grayscale image datasets demonstrate the effectiveness of the proposed model, achieving vastly lower latency (up to 16× less) and competitive or leading performance compared to other state-of-the-art image classification models on various domain-specific grayscale image classification datasets.

Index Terms— GCN, grayscale, image classification, MLP, low-latency

1. INTRODUCTION

As the demand and popularity of real-time systems increase, low-latency machine learning has become increasingly important. With more and more consumers interacting with machine learning models through the cloud, the speed at which those models can deliver results is critical. Consumers expect fast and accurate results; any latency can lead to a poor user experience. Moreover, low-latency machine learning is essential in real-time applications, such as autonomous vehicles or stock market trading, where decisions must be made quickly and accurately. In these scenarios, delays caused by high latency can result in severe consequences and even cause

inaccurate downstream calculations [1].

A particular instance where low-latency machine learning is needed is grayscale image classification. For example, a targeting system on a satellite is costly, and decisions must be made using SAR efficiently and accurately. Examples like this are where low-latency grayscale image classification comes into play. It is often the case that image classifiers work on RGB datasets and grayscale image datasets, but seldom do modern image classifiers focus solely on the grayscale setting. RGB models are overkill for the grayscale setting, as the grayscale problem allows us to focus on a single channel. Models focusing on grayscale image classification are naturally more efficient, as they can concentrate on a single channel rather than three. Thus, many image classifiers that generalize to the grayscale image classification are not truly optimized for the grayscale case. For these reasons, we present a lightweight grayscale image classifier capable of achieving up to 16× lower latency than other state-of-the-art machine learning models.

From a trustworthy visual data processing perspective, the demand for grayscale image classification requires data to be collected from various domains with high resolution and correctness so that we can train a robust machine learning model. Additionally, recent advancements in machine learning rely on convolutional neural networks, which often suffer from high computation costs, large memory requirements, and many network parameters, resulting in poor inference latency, poor scalability, and weak trustworthiness.

The inherent novelties of our model are the following: our proposed method is the first that vectorizes an image in a fully connected manner and inputs the resultant into a single-layer graph convolutional network (GCN). We also find that a single GCN layer is enough to stabilize the performance of our shallow model. Additionally, our proposed method benefits from a batch-wise attention term, allowing our shallow model to capture interdependencies between images and form connections for classification. Finally, by focusing on grayscale imagery, we can focus on a streamlined method for grayscale image classification rather than concentrating on the RGB setting. A result of these novelties is extremely low latency and high throughput for image classification.

With the recent technological advances, modern FPGAs contain many hardware resources [2], including DSPs, LUTs,

BRAMs, and URAMs. The programmable nature of FPGAs allows users to develop a customized data path and on-chip memory organization, leading to high-performance implementations. Consequently, FPGAs have emerged as an appealing option for executing time-sensitive machine learning tasks with reduced latency and power. For instance, FPGAs have been used for accelerating machine learning [3] and graph analytic tasks [4]. Given that our model is a lightweight image classifier, we find it suitable to be deployed on an FPGA. We can perform inference on the FPGA without returning the intermediate results to external memory. This ensures low-latency inference by capitalizing the fine-grained data parallelism inherent in FPGAs. In contrast, CPUs and GPUs exploit coarse-grained thread-level parallelism and have complex cache hierarchies, which are unsuitable for low-latency inference. Thus, this paper makes the following contributions:

- We present a lightweight, graph-based neural network for grayscale image classification. Specifically, we (1) apply image vectorization, (2) construct a graph for each batch of images and apply a single graph convolution, and (3) propose a weighted-sum mechanism to capture batch-wise dependencies.
- We implement our proposed method on FPGA, including the following design methodology: (1) a portable and parameterized hardware template using high-level synthesis, (2) layer-by-layer design to maximize runtime hardware resource utilization, and (3) a one-time data load strategy to reduce external memory accesses.
- Experiments show that our model achieves competitive or leading accuracy with respect to other popular state-of-the-art models while vastly reducing latency and model complexity.
- We implement our model on a state-of-the-art FPGA board, Xilinx Alveo U200. Compared with state-of-the-art GPU implementation, our FPGA implementation achieves $2.78\times$ speedup in latency and $2.1\times$ speedup in throughput.

2. PROBLEM DEFINITION

The problem is to design a lightweight system capable of handling high volumes of data with low latency. The solution should be optimized for performance and scalability while minimizing resource utilization, a necessary component of many real-time machine learning applications. The system should be able to process and respond to requests quickly, with minimal delays. High throughput and low latency are critical requirements for this system, which must handle many concurrent requests without compromising performance. We define latency and throughput in the following ways:

$$\text{Throughput} = \frac{\text{Total number of images processed}}{\text{Total inference time}}$$

$$\text{Latency} = \text{Total time for a single inference}$$

Latency refers to the total time (from start to finish) it takes to gather predictions for a model in one batch (a standard approach). A lightweight machine learning model aims to maximize throughput and accuracy while minimizing latency.

3. RELATED WORK

3.1. MLP Approaches

Our model combines various components of simple models and is inherently different from current works in low-latency image classification. Some recent architectures involve simple MLP-based models. Touvron et al. introduced ResMLP [5], an image classifier based solely on MLPs. ResMLP is trained in a self-supervised manner with patches interacting together. Touvron et al. highlight their model’s high throughput properties and accuracy. ResMLP uses patches from the image and alternates linear layers where patches interact and a two-layer feed-forward network where channels interact independently per patch. Additionally, MLP-Mixer [6] uses a similar patching method, which also attains competitive accuracy on RGB image datasets compared to other CNNs and transformer models. Our proposed method uses the results from a single-layer MLP to feed into a graph neural network, during which we skip the information from the three-channel RGB setting and only consider the single-channel grayscale problem. This is inherently different than the methods mentioned earlier, as they use patching approaches while we focus on the vectorization of pixels.

3.2. Graph Image Construction Methods

The dense graph mapping that utilizes each pixel as a node in a graph is used and mentioned by [7, 8]. For this paper, we employ the same terminology. Additionally, Zhang et al. presented a novel graph neural network architecture and examined its low-latency properties on the MSTAR dataset using the dense graph [9]. Our proposed method differs from dense graph methods, as we vectorize an image rather than using the entire grid as a graph.

Han et al. [10] form a graph from the image by splitting the image into patches, much like a transformer. A deep graph neural network learns on the patches similarly to a transformer but in a graph structure. Our structure does not form a graph where each patch is a node in a graph; instead, we create a graph from the resultant of a vectorized image passed through a single-layer MLP.

Mondal et al. proposed applying graph neural networks on a minibatch of images [11]. Mondal et al. claim that this method improves performance for adversarial attacks. We use the proposed method to stabilize the performance of a highly shallow model. The graph neural network, in this case, allows learning to be conducted in a graph form, connecting images containing similar qualities.

Besides the model proposed by Zhang et al., all the methods mentioned focus on the RGB setting. This is overkill for grayscale image classification. Focusing on a single channel allows us to develop a more streamlined solution rather than forcing a model to operate on RGB datasets and having the grayscale setting come as an afterthought. Doing so allows us to reduce computational costs.

4. OVERVIEW AND ARCHITECTURE

This section describes our model architecture (GECCO: Grayscale Efficient Channelwise Classification Operative). The overall process is summarized in Figure 1.

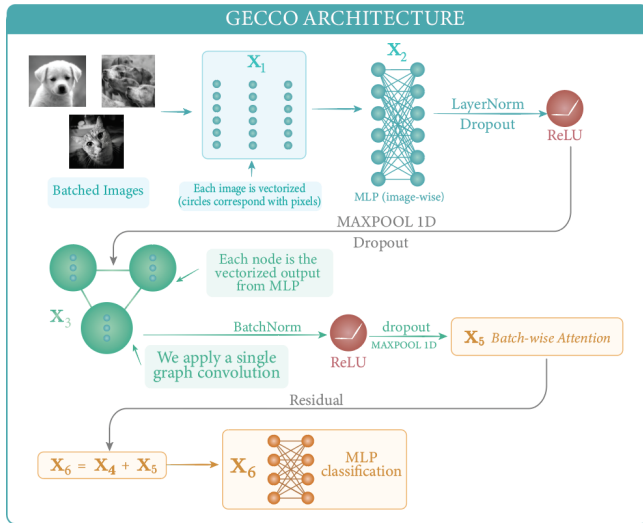


Fig. 1. GECCO Architecture

Overall Architecture. Many existing methods do not focus on the latency of their design and its implications. Additionally, the vast majority of image classification models focus on the performance of their work in the RGB setting, rarely citing the performance of datasets in various domains. We address these problems by presenting a novel architecture, focused on low latency and the grayscale image setting.

Our model vectorizes a batch of images, which allows us to use a fully connected layer pixel-wise for low computation time rather than the traditional reliance on convolutional neural networks. The proposed method uses the resultant from MLPs and constructs a graph batch-wise, where each node corresponds to the flattened image outputted from an MLP. We then apply a batch-wise attention term, inputted into an

MLP for classification. **Image Vectorization.** For each image in a batch, we view the image as a vector. For a tensor $\mathbf{X} \in \mathbb{R}^{B \times H \times W}$ where B is the batch size, H and W are the height and width of an image, we flatten the tensor to $\mathbf{X}_1 \in \mathbb{R}^{B \times (H \cdot W)}$. Viewing an image as a vector allows our model to skip the traditional convolutional neural network, which views the image as a grid and cuts computation time.

Simple MLP Layer. We input \mathbf{X}_1 into a linear MLP with output dimensionality D_{out} . Formally, $\text{MLP}(\mathbf{X}_1) \rightarrow \mathbf{X}_2 \in \mathbb{R}^{B \times D_{out}}$. Formally, $\text{MLP} = \sigma(\sum_j w_j x_j + b)$ where σ is a general activation term, each w is a learned weight vector, each x is a data vector, and b is a bias term. We then apply a standard layer norm and dropout functions. We use a standard activation function to \mathbf{X}_2 , followed by the standard dropout and MAXPOOL1D functions.

Graph Construction. Our graph construction consists of using each resultant vector from MLP as a node in a graph, such that the number of nodes in the graph corresponds with the number of images in a batch. This means that for each batch, a vectorized image is each node in the graph with feature size $\mathbb{R}^{D_{out}/2}$, and each image is connected to every other image in a batch. Formally, we calculate the adjacency matrix \mathbf{A} as $\mathbf{A}_{ij} = 1$, which connects all nodes. We then perform message passing amongst vectors, meaning the message that is aggregated from i 's graph neighborhood, given its neighbors j .

Graph Convolution. Our single GCN layer learns from similar features of images within its minibatch. Generally, a graph convolutional layer updates the representations of nodes by aggregating each node's neighbor's representation. It takes an input \mathbf{h}_i and maps an output $\mathbf{h}_i \mapsto \mathbf{h}'_i$ given its neighbors $\mathcal{N}_i = \{j \in \mathcal{V} \mid (j, i) \in \mathcal{E}\}$ where \mathbf{h}'_i is defined as

$$\mathbf{h}'_i = f_{\theta}(\mathbf{h}_i, \text{AGGREGATE}(\{\mathbf{h}_j \mid j \in \mathcal{N}_i\})).$$

In our case, the input for each node \mathbf{h}_i is the output from the MLP layer of a vectorized image. We claim that this component increases and stabilizes accuracy in the case of our simple MLP-based model. Section 5.2.1 presents a study of accuracy on MNIST with the graph convolutional layer varying. We find that the Residual Gated Graph Convolutional Network [12] outperforms in all categories, and thus, we use this as a backbone for our model.

From the result of inputting \mathbf{X}_2 into the previous dropout and MAXPOOL1D functions, we fix the resultant matrix \mathbf{X}_3 . From these functions, \mathbf{X}_3 inputs into a single-layer GCN with dimension $\mathbb{R}^{B \times D_{out}}$ and maps to the same output dimension $\mathbb{R}^{B \times D_{out}}$ where the output is denoted \mathbf{X}_4 .

Thus, we can denote a general GCN term output \mathbf{X}_4 . We then consider the output term layer as \mathbf{X}_4 as $\mathbf{X}_4 = \sigma(\mathbf{A}\mathbf{X}_3\mathbf{W})$ for the general GCN case where \mathbf{W} is a learned layer.

From the resultant matrix \mathbf{X}_4 , we apply a standard batch normalization term, activation function, and MAXPOOL1D functions.

The intuition behind this module is that it is helpful for such a shallow model to draw connections between images with similar properties batch-wise to stabilize accuracy. Adding graph convolutional layers past a single layer does not increase accuracy and deters performance for our model.

Batch-wise Attention, Residual Connections, & Output. Then, we propose the addition of a residual connection with batch-wise attention, defined as

$$\mathbf{X}_5 = \left(\frac{\sigma(\mathbf{X}_4 \mathbf{X}_4^\top)}{\sum_{i=1}^B \sum_{j=1}^B \sigma(\mathbf{X}_4 \mathbf{X}_4^\top)_{ij}} \right) \mathbf{X}_4$$

where σ is the standard sigmoid function. The batch-wise attention term allows the model to further capture similar features from each image to another batch-wise. Relating similar properties from images to each other boosts accuracy in our case; refer to our ablation study in Table 7.

The residual term is defined $\mathbf{X}_6 = \mathbf{X}_5 + \mathbf{X}_4$. The residual term allows our model to capture similar features while minimizing the risk of gradient explosion and retains information from the previous \mathbf{X}_4 step. By multiplying a softmax-like term with the output of a previous graph convolution, our intuition is that we weigh the correspondence of each pixel compared to other similar pixels within similar images batch-wise. This method differs from the standard query-key-value attention mechanism. It is more suitable to our case, as we allow batch-wise feature assimilation, allowing the model to capture similar features between images in a batch. In contrast, attention mechanisms focus on individual features, which may not be as effective in capturing batch-wise similarities. We then feed the residual term into an MLP for classification results.¹

5. EXPERIMENTS

5.1. Datasets

Datasets from several domains are examined to gauge the effectiveness of GECCO in diverse settings. We use the popular MNIST dataset [13], Fashion-MNIST [14], MSTAR, and CXR [15] summarized in the following manner:

- MNIST is a grayscale handwritten dataset with (28, 28) pixel image sizes and 10 different object categories. The training size for this dataset is 60000, and the testing size is 10000.
- Fashion-MNIST contains (28, 28) sized grayscale images from 10 categories with a training size of 60000, and a testing size of 10000.

¹We make our code publicly available at <https://github.com/GECCOProject/GECCO>

- MSTAR is a SAR ATR dataset with a training size of 2747 and testing size of 2425 SAR images of 10 different vehicle categories. We resize this dataset to (128, 128) pixels.
- CXR is a chest X-ray dataset containing 5863 X-ray images and 2 categories (Pneumonia/Normal). The images are (224, 224) pixels. The training size is 5216, and the testing size is 624.

5.2. Results

5.2.1. Backbone

For Table 1, we choose ResConv as the backbone of our model because it has the most desirable characteristics for applying a graph convolutional layer.

Table 1. Performance of GCN Layers Varying on MNIST

Convolutional Layer	Top-1 Accuracy	Throughput (imgs/ms)	Latency (ms)
GCN [16]	97.09%	54.58 ± 8.47	4.68 ± 0.72
TAGConv [17]	97.39%	58.39 ± 9.01	4.37 ± 0.67
SAGEConv [18]	97.77%	58.84 ± 8.98	4.32 ± 0.66
ChebConv [19]	97.50%	51.98 ± 8.65	4.91 ± 0.82
ResConv [12]	98.04%	62.44 ± 9.87	4.10 ± 0.65

5.2.2. Experimental Performance

Experimental performance includes the top-1 accuracy, inference throughput, and inference latency. We perform our inference batch-wise as a means to reduce latency. These metrics vary across each dataset.

In Tables 2, 3, 4, and 5, we present a summary of our findings. We report the best-performing accuracy, average throughputs, and latencies with their standard deviations. Our model outperforms every other model in terms of throughput and latency across all datasets, leads accuracy on the MSTAR dataset, and performs competitively in terms of accuracy on all datasets.

We perform the remaining experiments on a state-of-the-art NVIDIA RTX A5000 GPU. Additionally, we compare our model to the top-performing variants of VGG [20], the variant of the popular ViT [21], the ViT for small-sized datasets (SS-ViT) [22], FastViT [23], Swin Transformer [24], and ResNet [25] models. We use the open-source packages PyTorch and HuggingFace for model building and the PyTorch Op-Counter for operation counting. Performing the remaining experiments on the same hardware system is vital in fostering a fair comparison for each model.

Table 2. MNIST Performance

Model	Top-1 Accuracy	Throughput (imgs/ms)	Latency (ms)
Swin-T	98.30%	4.69 ± 0.21	54.53 ± 2.44
SS-ViT	98.09%	8.38 ± 1.42	30.46 ± 5.17
VGG16	99.54%	39.02 ± 4.98	6.55 ± 0.84
FastViT	98.44%	7.51 ± 0.51	34.05 ± 2.31
ResNet34	99.06%	12.88 ± 1.02	19.86 ± 1.57
GECCO	98.04%	62.44 ± 9.87	4.10 ± 0.65

Table 3. Fashion-MNIST Performance

Model	Top-1 Accuracy	Throughput (imgs/ms)	Latency (ms)
Swin-T	88.73%	4.58 ± 0.31	55.81 ± 3.78
SS-ViT	87.88%	8.27 ± 1.56	30.97 ± 5.83
VGG16	92.48%	24.98 ± 5.77	10.24 ± 2.36
FastViT	87.94%	7.28 ± 0.75	35.07 ± 3.63
ResNet34	88.50%	11.98 ± 1.05	21.35 ± 1.87
GECCO	88.09%	59.08 ± 9.04	4.32 ± 0.66

Table 4. MSTAR Performance

Model	Top-1 Accuracy	Throughput (imgs/ms)	Latency (ms)
Swin-T	86.04%	5.44 ± 0.37	46.98 ± 3.20
SS-ViT	95.61%	9.14 ± 1.72	27.97 ± 5.26
VGG16	93.13%	6.75 ± 1.34	37.89 ± 7.52
FastViT	91.78%	4.16 ± 0.52	61.44 ± 7.69
ResNet34	98.64%	12.44 ± 0.84	20.48 ± 1.39
GECCO	99.47%	67.17 ± 15.24	3.80 ± 0.86

Table 5. CXR Performance

Model	Top-1 Accuracy	Throughput (imgs/ms)	Latency (ms)
Swin-T	73.66%	1.08 ± 0.21	236.71 ± 46.09
SS-ViT	71.09%	4.09 ± 0.84	62.35 ± 12.85
VGG16	82.01%	3.03 ± 1.02	84.10 ± 28.43
FastViT	75.46%	4.24 ± 1.00	60.30 ± 14.24
ResNet34	78.31%	2.41 ± 0.44	105.84 ± 19.39
GECCO	79.87%	14.04 ± 3.19	18.05 ± 4.14

5.2.3. Model Complexity Metrics

Model complexity metrics for this paper include the number of multiply-accumulate operations, the number of model parameters, model size, and the number of layers. In other words, suppose accumulator a counts an operation of arbitrary $b, c \in \mathbb{R}$. We count the number of multiply-accumulate operations as $a \leftarrow a + (b \times c)$. Additionally, the layer count metric is an essential factor of latency. Increasing the number of layers will also improve the latency of a model’s inference. The goal of an effective machine learning model is to maximize throughput while minimizing the number of MACs and the number of layers, in our case.

We measure the model complexity of our model against other popular machine learning models that we have chosen in Table 6. Our model outperforms in all categories regarding our chosen model complexity metrics, highlighting its lightweightness.

Table 6. Model Complexity Metrics

Model	# MACs	# Parameters	Model Size (Mb)	# Layers
Swin-T	2.12×10^{10}	2.75×10^7	109.9	167
SS-ViT	1.55×10^{10}	4.85×10^6	19.62	79
VGG16	9.51×10^9	4.69×10^6	18.75	20
FastViT	7.16×10^8	4.02×10^6	16.1	226
ResNet34	4.47×10^9	2.13×10^7	85.1	92
GECCO	1.22×10^6	1.90×10^4	0.075	10

5.2.4. Ablation Study

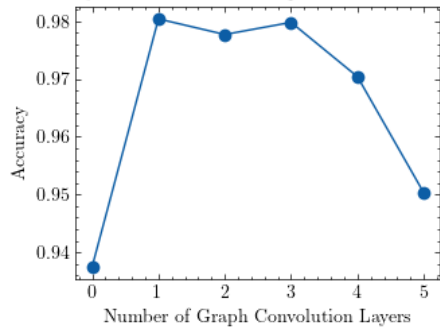
We perform an ablation study to verify that the components of our proposed model contribute positively to the overall accuracy.

Table 7. Ablation Study

Mini-batch GNN	Weighted Sum Residual Term	Accuracy on MNIST
✓	✓	98.02%
✗	✓	93.75%
✓	✗	92.17%
✗	✗	86.55%

Additionally, we find that only a single graph convolutional layer is enough to reduce the variance and increase the accuracy of our model. Refer to Figure 2.

Accuracy vs. Number of Graph Convolution Layers

**Fig. 2.** Accuracy on MNIST vs. Number of Graph Convolutional Layers

5.3. Discussion

Across multiple datasets, GECCO achieves leading or competitive accuracy compared to other state-of-the-art image classifiers. With respect to model complexity, it is clear that GECCO outperforms other machine learning models, highlighting our model’s low latency and lightweight properties.

It is difficult for our model to generalize to the RGB setting. We attribute this challenge to the vectorization process that our model uses. Learning on three channels poses a complexity challenge, as GECCO is very shallow and simple, thus making it challenging to learn on three separate channels.

Our proposed method does not make use of positional embeddings or class tokens. GECCO can learn essential features by the weighted residual term. Additionally, we tested the addition of positional embeddings and class tokens and found no improvement in accuracy across various datasets. We note that the X_5 residual term adds positional awareness to the model.

5.4. FPGA Implementation

We develop an accelerator for the proposed model on a state-of-the-art FPGA, Xilinx Alveo U200 board, to highlight the model’s efficiency and compatibility with hardware further. It has 3 Super Logic Regions (SLRs), 4 DDR memory banks, 1182k Look-up tables, 6840 DSPs, 75.9 Mb of BRAM, and 270 Mb of URAM. The FPGA kernels are developed using the Xilinx High-level Synthesis (HLS) tool to expedite the design process.

We perform the following optimizations for our FPGA design: (1) *Portable design*: We design a parameterized hardware template using HLS. It is portable to different FPGA platforms, including embedded and data-center FPGAs. (2) *Resource sharing*: The model is executed layer-by-layer. Each layer in the model is decomposed into basic kernel functions. The basic kernel functions, including matrix multiplication, elementwise activation, column-wise and row-wise summations, max pooling, and various other elementwise operations, are implemented separately and subsequently invoked within their corresponding layers. Due to the reuse of these fundamental kernel functions across multiple layers, FPGA resources are shared among the different layers, maximizing runtime hardware resource utilization. (3) *One-load strategy*: We employ a one-time data load strategy that enables us to load the required data from DDR only once. All other data required for the computations are stored in on-chip memory, reducing inference latency. Figure 3 illustrates the overall hardware architecture of our design.

We use the Vitis Analyzer tool to provide insights into resource utilization, latency, and throughput. Table 8 reports the results obtained for the MNIST dataset. Given the model’s compact design and resource efficiency, it can be accommodated within a single SLR. Hence, we deploy multiple accelerator instances across multiple SLRs, each with one instance. This increases the inference throughput. In table 8 shows the latency obtained for a single inference and the throughput achieved by running the design on 3 SLRs concurrently.

We compare our FPGA implementation with the baseline GPU implementation. The GPU baseline is executed on an NVIDIA RTX A5000 GPU, which operates at 1170 MHz and has a memory bandwidth of 768 GB/s. On the other hand, the FPGA operates at 300 MHz and has an external memory bandwidth of 77 GB/s. The GPU baseline is comparable with the FPGA in terms of the platform. Although the GPU has higher peak performance and memory bandwidth, our FPGA

implementation achieves a latency reduction of $2.78\times$ and a throughput improvement of $2.1\times$. This speedup is attributed to the optimizations mentioned above adopted in our implementation.

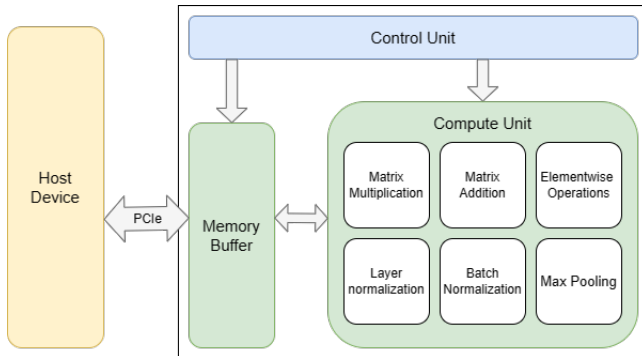


Fig. 3. Overview of Hardware Architecture

Table 8. Resource Utilization (per SLR), Latency, and Throughput for MNIST

Latency	1.47 ms
Throughput	130.61 imgs/ms
BRAMs	956 (22%)
DSPs	1226 (17%)
LUTs	459K (38%)
FFs	597K (25%)

6. CONCLUSION

This work presented a novel architecture based on MLPs and graph convolutional layers. We benchmarked our model on popular grayscale image datasets and highlighted the strength of our model in terms of its experimental performance and model complexity metrics. We emphasized the importance of a lightweight image classifier and examined the vast domain of grayscale image datasets. Overall, a lightweight and low-latency image classifier can improve the efficiency and effectiveness of various applications that rely on image processing.

Our model performs well in various domains, including general image classification, SAR ATR, and medical image classification. Additionally, we implement our model on FPGA to show that our model is hardware-friendly, which is an added benefit of any image classification model.

We presented the novelties of our model, which include viewing an image as a vector in a fully connected manner and inputting the resultant into a single-layer GCN. We also found that graph neural networks can increase the accuracy and reduce the variance in performance of shallow models like ours. Additionally, a simple batch-wise attention term allows our shallow model to capture interdependencies between images and form connections for classification. These novelties result in a highly low latency and high throughput model.

7. REFERENCES

- [1] Kaoru Ota, Minh Son Dao, Vasileios Mezaris, and Francesco G. B. De Natale, “Deep learning for mobile multimedia: A survey,” *ACM Trans. Multimedia Comput. Commun. Appl.*, vol. 13, no. 3s, jun 2017.
- [2] Tan Nguyen, Samuel Williams, Marco Siracusa, Colin MacLean, Douglas Doerfler, and Nicholas J. Wright, “The performance and energy efficiency potential of fpga in scientific computing,” in *2020 IEEE/ACM Performance Modeling, Benchmarking and Simulation of High Performance Computer Systems (PMBS)*, 2020, pp. 8–19.
- [3] Fahad Siddiqui, Sam Amiri, Umar Ibrahim Minhas, Tiantai Deng, Roger Woods, Karen Rafferty, and Daniel Crookes, “Fpga-based processor acceleration for image processing applications,” *Journal of Imaging*, vol. 5, no. 1, pp. 16, 2019.
- [4] Bingyi Zhang, Hanqing Zeng, and Viktor Prasanna, “Graphagile: An fpga-based overlay accelerator for low-latency gnn inference,” *IEEE Transactions on Parallel and Distributed Systems*, vol. 34, no. 9, pp. 2580–2597, 2023.
- [5] Hugo Touvron, Piotr Bojanowski, Mathilde Caron, Matthieu Cord, Alaaeldin El-Nouby, Edouard Grave, Gautier Izacard, Armand Joulin, Gabriel Synnaeve, Jakob Verbeek, and Hervé Jégou, “Resmlp: Feed-forward networks for image classification with data-efficient training,” 2021.
- [6] Ilya Tolstikhin, Neil Houlsby, Alexander Kolesnikov, Lucas Beyer, Xiaohua Zhai, Thomas Unterthiner, Jessica Yung, Andreas Steiner, Daniel Keysers, Jakob Uszkoreit, Mario Lucic, and Alexey Dosovitskiy, “Mlp-mixer: An all-mlp architecture for vision,” 2021.
- [7] Benjamin Sanchez-Lengeling, Emily Reif, Adam Pearce, and Alexander B. Wiltschko, “A gentle introduction to graph neural networks,” *Distill*, 2021, <https://distill.pub/2021/gnn-intro>.
- [8] Naman Goyal and David Steiner, “Graph neural networks for image classification and reinforcement learning using graph representations,” 2022.
- [9] Bingyi Zhang, Rajgopal Kannan, Viktor Prasanna, and Carl Busart, “Accurate, low-latency, efficient sar automatic target recognition on fpga,” in *2022 32nd International Conference on Field-Programmable Logic and Applications (FPL)*. Aug. 2022, IEEE.
- [10] Kai Han, Yunhe Wang, Jianyuan Guo, Yehui Tang, and Enhua Wu, “Vision gnn: An image is worth graph of nodes,” 2022.
- [11] Arnab Kumar Mondal, Vineet Jain, and Kaleem Siddiqi, “Mini-batch graphs for robust image classification,” 2021.
- [12] Xavier Bresson and Thomas Laurent, “Residual gated graph convnets,” 2018.
- [13] Yann LeCun, Corinna Cortes, and CJ Burges, “Mnist handwritten digit database,” *ATT Labs [Online]*. Available: <http://yann.lecun.com/exdb/mnist>, vol. 2, 2010.
- [14] Han Xiao, Kashif Rasul, and Roland Vollgraf, “Fashion-mnist: a novel image dataset for benchmarking machine learning algorithms,” 2017.
- [15] Daniel Kermany, “Labeled optical coherence tomography (oct) and chest x-ray images for classification,” 2018.
- [16] Thomas N. Kipf and Max Welling, “Semi-supervised classification with graph convolutional networks,” 2017.
- [17] Jian Du, Shanghang Zhang, Guanhang Wu, Jose M. F. Moura, and Soumya Kar, “Topology adaptive graph convolutional networks,” 2018.
- [18] William L. Hamilton, Rex Ying, and Jure Leskovec, “Inductive representation learning on large graphs,” 2018.
- [19] Michaël Defferrard, Xavier Bresson, and Pierre Vandergheynst, “Convolutional neural networks on graphs with fast localized spectral filtering,” 2017.
- [20] Karen Simonyan and Andrew Zisserman, “Very deep convolutional networks for large-scale image recognition,” 2015.
- [21] Alexey Dosovitskiy, Lucas Beyer, Alexander Kolesnikov, Dirk Weissenborn, Xiaohua Zhai, Thomas Unterthiner, Mostafa Dehghani, Matthias Minderer, Georg Heigold, Sylvain Gelly, Jakob Uszkoreit, and Neil Houlsby, “An image is worth 16x16 words: Transformers for image recognition at scale,” 2021.
- [22] Seung Hoon Lee, Seunghyun Lee, and Byung Cheol Song, “Vision transformer for small-size datasets,” *CoRR*, vol. abs/2112.13492, 2021.
- [23] Pavan Kumar Anasosalu Vasu, James Gabriel, Jeff Zhu, Oncel Tuzel, and Anurag Ranjan, “Fastvit: A fast hybrid vision transformer using structural reparameterization,” 2023.
- [24] Ze Liu, Yutong Lin, Yue Cao, Han Hu, Yixuan Wei, Zheng Zhang, Stephen Lin, and Baining Guo, “Swin transformer: Hierarchical vision transformer using shifted windows,” 2021.
- [25] Kaiming He, Xiangyu Zhang, Shaoqing Ren, and Jian Sun, “Deep residual learning for image recognition,” 2015.